Spectral Coherence Along a Lidar-Anemometer Beam

Kristensen, Leif; Kirkegaard, Peter; Mann, Jakob; Mikkelsen, Torben; Nielsen, Morten; Sjöholm, Mikael

Publication date:
2010

Document Version
Publisher's PDF, also known as Version of record

Spectral Coherence Along a Lidar-Anemometer Beam

Risø-R-Report

Leif Kristensen, Peter Kirkegaard, Jakob Mann, Torben Mikkelsen, Morten Nielsen, Mikael Sjöholm
Risø-R-1744(EN)
October 2010

Risø DTU
National Laboratory for Sustainable Energy

Author: Leif Kristensen, Peter Kirkegaard, Jakob Mann, Torben Mikkelsen, Morten Nielsen, Mikael Sjöholm
Title: Spectral Coherence Along a Lidar-Anemometer Beam
Division: Wind Energy Division

Abstract (max. 2000 char.):
The theory of measuring the spectral coherence by means of a lidar anemometer has been outlined. It is based on the assumption that the turbulent velocity field can be considered statistically locally isotropic and on the validity of Taylor's hypothesis. This implies that the longitudinal coherence cannot be predicted realistically. Special emphasis has been placed on the effect of line average along the beam. One section has been devoted to the effect of spectral aliasing, which may cause severe problems in the interpretation of measured data. This work is considered the theoretical background for the understanding of the coherences calculated on basis of real date.

Risø-R-1744(EN)
October 2010

ISSN 0106-2840
ISBN 978-87-550-3840-0

Contract no.:

Group's own reg. no.:
1130408-01

Sponsorship:
Danish Strategic Research Council, grant no. 2104-05-0076

Cover :

Pages: 20
Tables: 0
References: 7

Information Service Department
Risø National Laboratory for Sustainable Energy
Technical University of Denmark
P.O.Box 49
DK-4000 Roskilde
Denmark
Telephone +45 46774005
bibl@risoe.dtu.dk
Fax +45 46774013
www.risoe.dtu.dk

Contents

1 Introduction

The development on anemometers based on the lidar (Light Detection and Ranging), i.e. a pulsed laser, offers a unique opportunity to determine wind speeds at many points simultaneously. Each pulse, which is approximately of a Gaussian form in time, is reflected by aerosols along the beam and received at the point where the pulses are emitted. The Doppler shift of the returned signal is proportional to the component of the air velocity along the beam. By gating this received continuous signal in a number of time interval gates we obtain from each gate the velocity corresponding to the distance equal half the delay after the pulse emission multiplied by the velocity of light c. This time-of-flight technique is illustrated in Fig. 1, where T is the time elapsed after the emission of a pulse. The distance D is equal to $c/2$ multiplied by the time difference of two neighboring sampling periods.

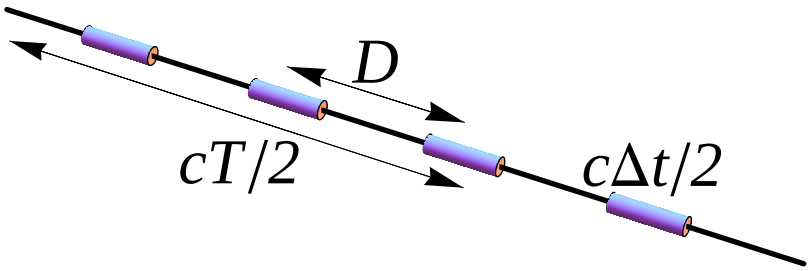

Figure 1. Sketch of a lidar anemometer with range gauges separated by the distance D. The duration Δt of each range gate corresponds to the spatial length $c\Delta t/2$. The start of a range gate, in this case the third, is $T - \Delta t/2$, which means that the corresponding position of the range-gate center in space is $cT/2$ along the beam.

Obviously, the measured velocities are not point measurements. They are observed through a line filter along the beam. This filter is composed of the averaging by the range gates and of the laser pulse-form. This filtering will be the main subject. We will also determine the effect of aliasing, which is determined by the time interval between emission of laser pulses. We will discuss the mathematical tools for predicting and interpretation of spectral coherence measured by a lidar anemometer. However, first we will, to have a simple reference, derive the coherence under the assumption that the velocities are point measurements.

2 Point Measurements

With reference to Fig. 2, the laser beam has the direction of the unit vector $\boldsymbol{t}$, which we define as the $\boldsymbol{i}_1^\circ$ direction in a Cartesian coordinate system. The $\boldsymbol{i}_3^\circ$ is defined as

$$\boldsymbol{i}_3^\circ = \frac{\boldsymbol{i}_1^\circ \times \boldsymbol{U}}{|\boldsymbol{i}_1^\circ \times \boldsymbol{U}|}, \tag{1}$$

where $\boldsymbol{U}$ is the direction of the mean-wind vector. Then the final unit vector in the Cartesian coordinate system becomes

$$\boldsymbol{i}_2^\circ = \boldsymbol{i}_3^\circ \times \boldsymbol{i}_1^\circ. \tag{2}$$

The displacement vector $\boldsymbol{D} = D\boldsymbol{i}_1^\circ$ is in the direction of the beam. However, it seems convenient, when applying Taylor's hypothesis, to rotate the coordinate system the angle $\pi/2 - \beta$, where β is defined such that the angle between the beam and the mean-wind direction is $\pi - \beta$. This is illustrated in Fig. 2. In this way it becomes easier to determine the coherence since the angle between the mean-wind direction and the projected displacement $\boldsymbol{D}' = D'\,\boldsymbol{i}_1$, where $D' = D\sin\beta$, becomes $\pi/2$. This is a result of Taylor's hypothesis since the coherence is then independent of the time lag $D \times \cos\beta/U$.

The new coordinate system is defined by the unit vectors

$$\left\{ \begin{array}{c} \boldsymbol{i}_1 \\ \boldsymbol{i}_2 \\ \boldsymbol{i}_3 \end{array} \right\} = \left\{ \begin{array}{c} \boldsymbol{i}_1^\circ \sin\beta + \boldsymbol{i}_2^\circ \cos\beta \\ -\boldsymbol{i}_1^\circ \cos\beta + \boldsymbol{i}_2^\circ \sin\beta \\ \boldsymbol{i}_3^\circ \end{array} \right\}. \tag{3}$$

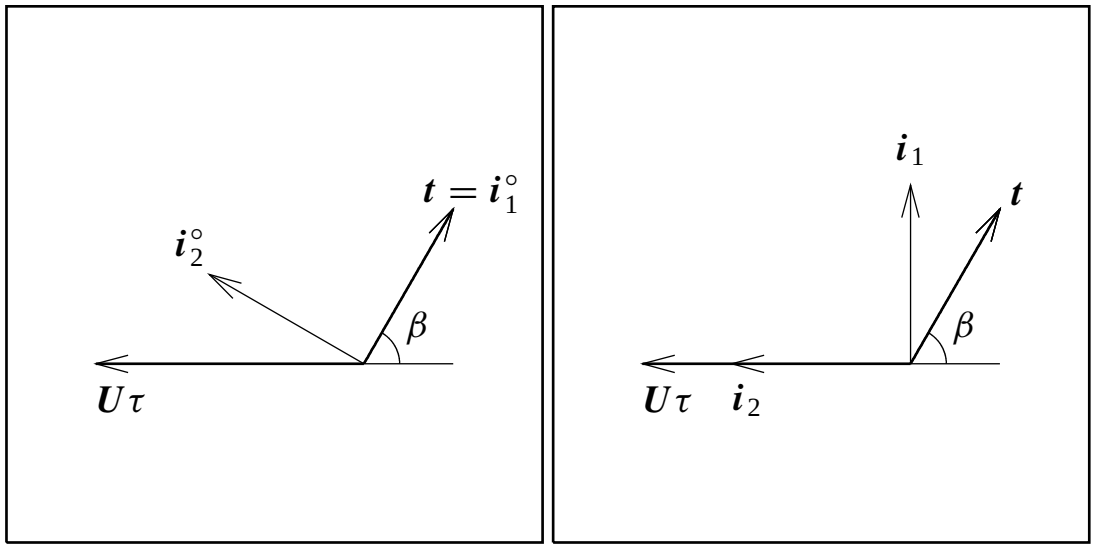

Figure 2. Left frame illustrates the physical setup. The right frame shows the rotated coordinate system.

The covariance tensor is in our case

$$R_{ij}(\boldsymbol{r},\tau) = R_{ij}(D'\boldsymbol{i}_1 - U\tau\boldsymbol{i}_2, 0) \equiv R_{ij}(D'\boldsymbol{i}_1 - U\tau\boldsymbol{i}_2). \tag{4}$$

The temporal Fourier transform is the cross-spectral tensor

$$\chi_{ij}^\circ(D',\omega) = \frac{1}{2\pi}\int_{-\infty}^{\infty} R_{ij}(D'\boldsymbol{i}_1 - U\tau\boldsymbol{i}_2)\mathrm{e}^{-\mathrm{i}\,\omega\tau}\,\mathrm{d}\tau. \tag{5}$$

We express this function in terms of the spectral velocity tensor $\Phi_{ij}(\boldsymbol{k})$ by using the transform

$$R_{ij}(\boldsymbol{r}) = \int \Phi_{ij}(\boldsymbol{k})\,\mathrm{e}^{\mathrm{i}\,\boldsymbol{k}\cdot\boldsymbol{r}}\,\mathrm{d}^3k. \tag{6}$$

In the following equation chain we use this on $\chi^{\circ}_{ij}(D', \omega)$ as given by (5):

$$\begin{aligned}
\chi^{\circ}_{ij}(D', \omega) &= \frac{1}{2\pi} \int_{-\infty}^{\infty} \mathrm{e}^{-\mathrm{i}\,\omega\tau}\, \mathrm{d}\tau \int \Phi_{ij}(\boldsymbol{k})\, \mathrm{e}^{\mathrm{i}\,(D'k_1 - U\tau k_2)}\, \mathrm{d}^3k \\
&= \int \Phi_{ij}(\boldsymbol{k})\, \mathrm{e}^{\mathrm{i}\,D'k_1}\, \mathrm{d}^3k \frac{1}{2\pi} \int_{-\infty}^{\infty} \mathrm{e}^{-\mathrm{i}\,(\omega + Uk_2)\tau}\, \mathrm{d}\tau \\
&= \int \Phi_{ij}(\boldsymbol{k})\, \mathrm{e}^{\mathrm{i}\,D'k_1} \delta(\omega + Uk_2)\, \mathrm{d}^3k, \qquad (7)
\end{aligned}$$

where $\delta(x)$ is Dirac's delta function.

To determine the coherence between the velocity components along the laser beam $\boldsymbol{t}$ we project

$$\Phi_{ij}(\boldsymbol{k}) = \frac{E(k)}{4\pi k^2} \left\{ \delta_{ij} - \frac{k_i k_j}{k^2} \right\} \qquad (8)$$

on the outer product of

$$\boldsymbol{t} = \sin\beta \boldsymbol{i}_1 - \cos\beta \boldsymbol{i}_2 \qquad (9)$$

with itself. The corresponding tensor element is

$$\Phi_{tt} = \frac{E(k)}{4\pi k^2} \left\{ 1 - \frac{(k_1 \sin\beta - k_2 \cos\beta)^2}{k^2} \right\}. \qquad (10)$$

We use the energy spectrum for local isotropy

$$E(k) = \alpha\, \varepsilon^{2/3}\, k^{-5/3}, \qquad (11)$$

where ε is the rate of dissipation of specific, kinetic energy and $\alpha \simeq 1.71$ the dimensionless Kolmogorov constant [see discussion by Kristensen et al. (1989, p. 162)].

With these tools we get the cross spectrum

$$\chi^{\circ}_{tt}(D', \omega) = \int \frac{E(k)}{4\pi k^2} \left\{ 1 - \frac{(k_1 \sin\beta - k_2 \cos\beta)^2}{k^2} \right\} \mathrm{e}^{\mathrm{i}\,D'k_1}\, \delta(\omega + Uk_2)\, \mathrm{d}^3k. \qquad (12)$$

Integrating over k_2, we obtain

$$\begin{aligned}
&\chi^{\circ}_{tt}(D', \omega) = \\
&\frac{1}{4\pi U} \int_{-\infty}^{\infty} \mathrm{e}^{\mathrm{i}\,D'k_1}\, \mathrm{d}k_1 \int_{-\infty}^{\infty} \mathrm{d}k_3 \frac{E\left(\sqrt{\omega^2/U^2 + k_1^2 + k_3^2}\right)}{\omega^2/U^2 + k_1^2 + k_3^2} \\
&\qquad \times \left\{ 1 - \frac{((\omega/U)\cos\beta + k_1 \sin\beta)^2}{\omega^2/U^2 + k_1^2 + k_3^2} \right\}. \qquad (13)
\end{aligned}$$

We transform (13) to polar integration by

$$\left\{ \begin{array}{c} k_1 \\ k_3 \end{array} \right\} = \left\{ \begin{array}{c} K\cos\Theta \\ K\sin\Theta \end{array} \right\} \tag{14}$$

so that (13) becomes

$$\chi^{\circ}_{tt}(D',\omega) = \frac{1}{4\pi U}\int_0^{\infty} \frac{E\left(\sqrt{\omega^2/U^2+K^2}\right)}{\omega^2/U^2+K^2} K\,\mathrm{d}K$$

$$\int_0^{2\pi} \left\{ 1 - \frac{((\omega/U)\cos\beta + K\sin\beta\cos\Theta)^2}{\omega^2/U^2+K^2} \right\} \mathrm{e}^{\mathrm{i}\,D'K\cos\Theta}\mathrm{d}\Theta. \tag{15}$$

We rewrite this equation in the following way

$$\chi^{\circ}_{tt}(D',\omega) = \frac{1}{2\pi U}\int_0^{\infty} \frac{E\left(\sqrt{\omega^2/U^2+K^2}\right)}{\omega^2/U^2+K^2} K\,\mathrm{d}K$$

$$\int_0^{\pi} \left\{ 1 - \frac{((\omega/U)\cos\beta + K\sin\beta\cos\Theta)^2}{\omega^2/U^2+K^2} \right\} \mathrm{e}^{\mathrm{i}\,D'K\cos\Theta}\mathrm{d}\Theta.$$

$$= \frac{1}{\pi U}\int_0^{\infty} \frac{E\left(\sqrt{\omega^2/U^2+K^2}\right)}{\omega^2/U^2+K^2} K\,\mathrm{d}K$$

$$\times \int_0^{\pi/2} \left\{ \left(1 - \frac{(\omega/U)^2\cos^2\beta + K^2\sin^2\beta\cos^2\Theta}{(\omega/U)^2+K^2} \right) \cos\left(D'K\cos\Theta\right) \right.$$

$$\left. - 2\mathrm{i}\,\frac{(\omega/U)K\cos\beta\sin\beta\cos\Theta}{(\omega/U)^2+K^2} \sin\left(D'K\cos\Theta\right) \right\} \mathrm{d}\Theta \tag{16}$$

The integration over Θ can be expressed in terms of Bessel functions since

$$\frac{1}{\pi}\int_0^{\pi/2} \cos(x\cos\Theta)\mathrm{d}\Theta = \frac{1}{2}J_{\circ}(x), \tag{17}$$

$$\frac{1}{\pi}\int_0^{\pi/2} \cos^2\Theta\cos(x\cos\Theta)\mathrm{d}\Theta = \frac{1}{2}\left\{ J_{\circ}(x) - \frac{J_1(x)}{x} \right\}, \tag{18}$$

and

$$\frac{1}{\pi}\int_0^{\pi/2}\cos\Theta\sin(x\cos\Theta)\mathrm{d}\Theta=\frac{1}{2}J_1(x). \tag{19}$$

$$\chi^{\circ}_{tt}(D',\omega)=\frac{1}{2U}\int_0^{\infty}\frac{E\left(\sqrt{\omega^2/U^2+K^2}\right)}{(\omega^2/U^2+K^2)^2}K\mathrm{d}K$$

$$\left\{\left(\frac{\omega^2}{U^2}\sin^2\beta+K^2\cos^2\beta\right)J_{\circ}(D'K)+K^2\left(\sin^2\beta-\mathrm{i}\,\frac{\omega}{U}D'\sin(2\beta)\right)\frac{J_1(D'K)}{D'K}\right\}. \tag{20}$$

Applying (11) and using the notation $(s_{\circ},s)=(\omega D'/U,\,K\,D')$, we get

$$\chi^{\circ}_{tt}(D',\omega)=\frac{\alpha\varepsilon^{2/3}D'^{5/3}}{2U}\int_0^{\infty}\frac{s\mathrm{d}s}{(s_{\circ}^2+s^2)^{17/6}}$$

$$\left\{(s_{\circ}^2\sin^2\beta+s^2\cos^2\beta)J_{\circ}(s)+(\sin^2\beta-\mathrm{i}\,s_{\circ}\sin(2\beta))sJ_1(s)\right\} \tag{21}$$

We can carry out this integral in terms of Bessel Functions by means of the general integral (Olver 1964, (eq. 11.4.44, p. 488))

$$\int_0^{\infty}\frac{s^{p+1}J_p(as)\mathrm{d}s}{(s_{\circ}^2+s^2)^{\mu+1}}=\frac{a^{\mu}s_{\circ}^{p-\mu}}{2^{\mu}\Gamma(\mu+1)}K_{p-\mu}(as_{\circ}) \tag{22}$$

and the relations (Olver 1964, (eqs. 9.6.26, p. 376, and 9.6.2, p. 375))

$$K_{-p}(x)=K_p(x), \tag{23}$$

$$K_{p+1}(x)=\frac{2p}{x}K_p(x)+K_{p-1}(x). \tag{24}$$

This leads to

$$\int_0^{\infty}\frac{sJ_{\circ}(s)\mathrm{d}s}{(s_{\circ}^2+s^2)^{17/6}}=\frac{K_{11/6}(s_{\circ})}{(2s_{\circ})^{11/6}\Gamma(17/6)}, \tag{25}$$

$$\int_0^{\infty}\frac{s^2J_1(s)\mathrm{d}s}{(s_{\circ}^2+s^2)^{17/6}}=\frac{K_{5/6}(s_{\circ})}{2(2s_{\circ})^{5/6}\Gamma(17/6)}, \tag{26}$$

and, by a little manipulation,

$$\int_0^{\infty}\frac{s^3J_{\circ}(s)\mathrm{d}s}{(s_{\circ}^2+s^2)^{17/6}}=\frac{K_{5/6}(s_{\circ})-(s_{\circ}/2)K_{1/6}(s_{\circ})}{(2s_{\circ})^{5/6}\Gamma(17/6)}. \tag{27}$$

Inserting (25), (26), and (27) in (21), we get

$$\begin{aligned}\chi^{\circ}_{tt}(D',\omega) &= \frac{\alpha\varepsilon^{2/3}D'^{5/3}}{2U}\frac{1}{(2s_\circ)^{5/6}}\frac{1}{\Gamma(17/6)} \\ &\times\Big\{(2/3)\sin^2\beta\left(2K_{5/6}(s_\circ)+(3/4)s_\circ K_{1/6}(s_\circ)\right) \\ &+ (1/2)\cos^2\beta\left(2K_{5/6}(s_\circ)-s_\circ K_{1/6}(s_\circ)\right) \\ &- \mathrm{i}\cos\beta\sin\beta\, s_\circ K_{5/6}(s_\circ)\Big\}. \end{aligned} \tag{28}$$

Using the limiting form by Olver (1964, (eq. 9.6.9, p. 375)) for small arguments

$$K_p(x) \sim \frac{1}{2}\Gamma(p)\left(\frac{x}{2}\right)^{-p} \tag{29}$$

we get

$$\begin{aligned}\chi^{\circ}_{tt}(D',\omega)_{s_\circ\to 0} &= \frac{\alpha\varepsilon^{2/3}D'^{5/3}}{2U}\frac{1}{(2s_\circ)^{5/6}}\frac{1}{\Gamma(17/6)} \\ &\times\frac{1}{2}\Gamma(5/6)\left(\frac{s_\circ}{2}\right)^{-5/6}\left\{\frac{4}{3}\sin^2\beta+\cos^2\beta\right\}. \end{aligned} \tag{30}$$

We obtain the coherence as the absolute square of the ratio $\chi^{\circ}_{tt}(D',\omega)/\chi^{\circ}_{tt}(D',\omega)_{s_\circ\to 0}$:

$$\begin{aligned}\mathrm{coh}(\beta,\omega D/U) &= \frac{4(s_\circ/2)^{5/3}}{\Gamma^2(5/6)}\times \\ &\left\{\frac{[((4/3)\sin^2\beta+\cos^2\beta)K_{5/6}(s_\circ)+(1/2)(\sin^2\beta-\cos^2\beta)s_\circ K_{1/6}(s_\circ)]^2}{[(4/3)\sin^2\beta+\cos^2\beta]^2}\right. \\ &\left.+\frac{\cos^2\beta\sin^2\beta\, s_\circ^2 K_{5/6}^2(s_\circ)}{[(4/3)\sin^2\beta+\cos^2\beta]^2}\right\} \end{aligned} \tag{31}$$

where $s_\circ = \omega D'/U = \omega D\sin\beta/U$. The coherence is shown in Fig. 3 for selected values of β. We see that Taylor's hypothesis implies that the coherence is unity for $\beta = 0$ as expected and pointed out by Kristensen & Jensen (1979). They also derived the coherence for the special case $\beta = \pi/2$.

3 Line Averaging

The line averaging along the beam in the direction of the unit vector $\boldsymbol{t}$ consists of two elements: the durations of the lidar pulse and of the gate opening.

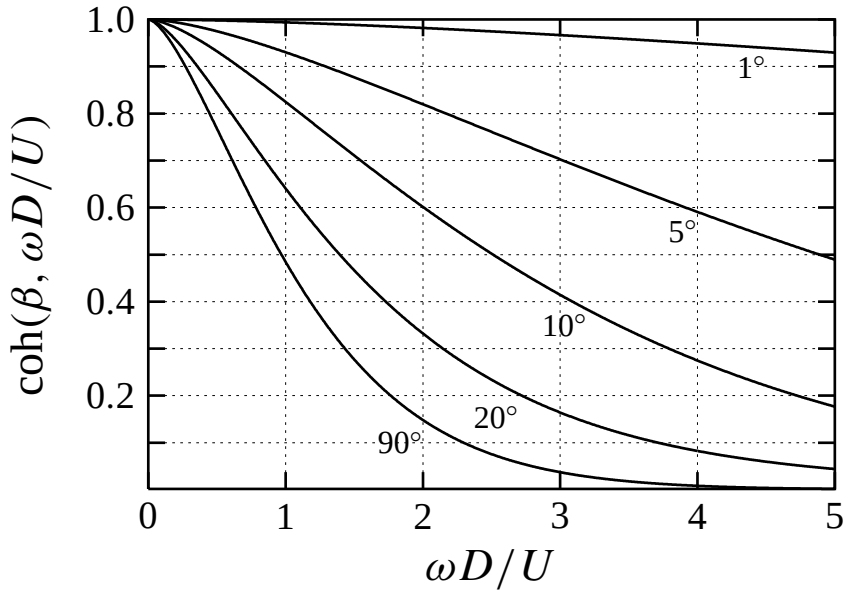

Figure 3. The coherence (31) for selected values of β.

For a pulsed laser it can be assumed that the temporal form of the pulse is a Gaussian, while the gate-opening window often is characterized by being constant in time in its entire duration Δt. Both the pulse and the gate are normalized, i.e. with their integrals equal to unity. Figure 4 shows the situation. The range gating is carried out by averaging the return signal from the Gaussian pulse* over the time from $T - \Delta t/2$ to $T + \Delta t/2$.

In this time interval we get the contribution from the distance $x = ct/2$

$$h(T, \Delta t, \sigma, x) = \frac{1}{\Delta t} \int_{T-\Delta t/2}^{T+\Delta t/2} \exp\left(-\frac{(x - ct'/2)^2}{2\sigma^2} \right) \frac{\mathrm{d}t'}{\sqrt{2\pi}\sigma}, \tag{32}$$

where σ standard deviation of the Gaussian pulse.

Since it is more convenient to work in spatial rather than temporal coordinates, we introduce the notation

$$\left\{ \begin{array}{c} x' \\ R \\ L \end{array} \right\} = \left\{ \begin{array}{c} ct'/2 \\ cT/2 \\ c\Delta t/2 \end{array} \right\} \tag{33}$$

and get

$$h(R, L, \sigma, x) = \frac{1}{L} \int_{R-L/2}^{R+L/2} \exp\left(-\frac{(x - x')^2}{2\sigma^2} \right) \frac{\mathrm{d}x'}{\sqrt{2\pi}\sigma}$$

*Since the pulse must travel out and back, the detected signal has effectively traveled with half the speed of light $c/2$.

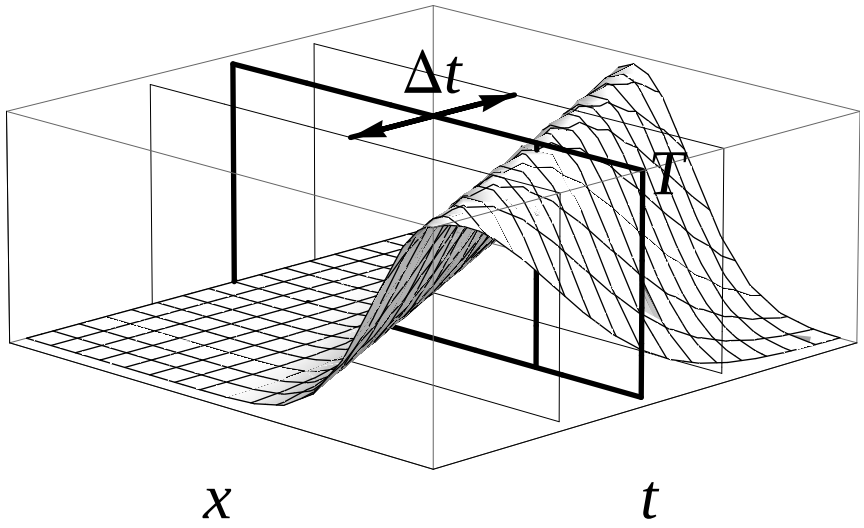

Figure 4. A pulse of Gaussian shape progressing in the x-direction as function of time t. The Gaussian wave is averaged over the interval $[T - \Delta t/2, T + \Delta t/2]$.

$$= \frac{1}{L}\int_{-L/2}^{L/2} \exp\left(-\frac{(R-x-x')^2}{2\sigma^2}\right)\frac{\mathrm{d}x'}{\sqrt{2\pi}\sigma}. \tag{34}$$

The Fourier transform

$$\widehat{h}(R,L,\sigma,k) = \int_{-\infty}^{\infty} h(R,L,\sigma,x)\,\mathrm{e}^{\mathrm{i}kx}\mathrm{d}x = \mathrm{e}^{\mathrm{i}kR}\,\mathrm{sinc}\left(\frac{kL}{2}\right)\exp\left(-\frac{\sigma^2k^2}{2}\right) \tag{35}$$

is obtained by reversing the order of integration and the transfer function thus becomes

$$H(\{L,\sigma\},\boldsymbol{k}) = \mathrm{sinc}^2\left(\frac{\boldsymbol{k}\cdot\boldsymbol{t}L}{2}\right)\exp\left(-(\boldsymbol{k}\cdot\boldsymbol{t})^2\sigma^2\right). \tag{36}$$

This approach was also used by Frehlich (1997) and by Banakh & Smalikho (1997). It is convenient to use an approximate form of this function,

$$H(\ell,\boldsymbol{k}) = \exp\left(-(\boldsymbol{k}\cdot\boldsymbol{t})^2\ell^2\right), \tag{37}$$

where

$$\ell = \sqrt{\frac{L^2}{12}+\sigma^2}. \tag{38}$$

It is easily verified that the approximation is exact up to fourth order in $|\boldsymbol{k}|L$ [†].

[†] An alternative, but somewhat inconvenient, approximation could be $H(\ell,\boldsymbol{k}) = \mathrm{sinc}^2(\boldsymbol{k}\cdot\boldsymbol{t}\,\ell/2)$ with $\ell = \sqrt{L^2+12\sigma^2}$

So far we have assumed that the gate is uniform. This is very often the case, at least approximately. However, the gate window may also be tapered (Jean-Pierre Cariou, 2010, private communication, Leosphere, Paris). If we assume, as illustrated in Fig. 5, a truncated Gaussian tapering of the form

$$W(x) = \begin{cases} \frac{1}{\sqrt{2\pi}(L/q)} \exp\left(-q^2 \frac{x^2}{2L^2}\right) & |x| \le L/2 \\ 0 & |x| > L/2 \end{cases}, \tag{39}$$

where q is a dimensionless parameter to be determined, (34) must be replaced by

$$\begin{aligned} h(R, L, \sigma, x) &= \int_{-L/2}^{L/2} \frac{1}{\sqrt{2\pi}(L/q)} \exp\left(-q^2 \frac{x'^2}{2L^2}\right) \exp\left(-\frac{(R-x-x')^2}{2\sigma^2}\right) \frac{\mathrm{d}x'}{\sqrt{2\pi}\sigma} \\ &\approx \int_{-\infty}^{\infty} \frac{1}{\sqrt{2\pi}(L/q)} \exp\left(-q^2 \frac{x'^2}{2L^2}\right) \exp\left(-\frac{(R-x-x')^2}{2\sigma^2}\right) \frac{\mathrm{d}x'}{\sqrt{2\pi}\sigma} \\ &= \frac{1}{\sqrt{2\pi\left(\sigma^2 + L^2/q^2\right)}} \exp\left(-\frac{(R-x)^2}{2\left(\sigma^2 + L^2/q^2\right)}\right). \end{aligned} \tag{40}$$

The transfer function is again of the form (37) with

$$\ell = \sqrt{\frac{L^2}{q^2} + \sigma^2}. \tag{41}$$

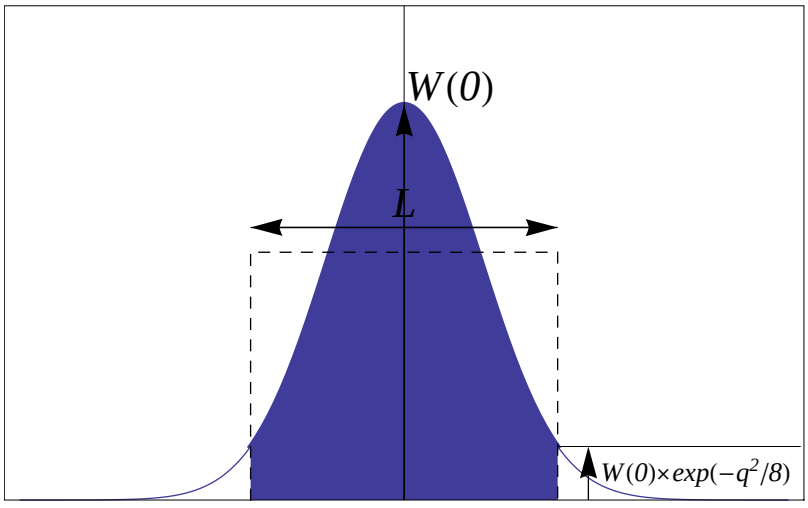

Figure 5. The tapered Gauss gate (39).

We base the derivation of the filtered coherence in (13) and the transfer function

$$H(\ell, \boldsymbol{k}) = \exp\left(-(k_1 \sin\beta - k_2 \cos\beta)^2 \ell^2\right). \tag{42}$$

Here we use the notation $k_2 = -\omega/U$ (see (12)).

With this form of the filter the filtered cross spectrum can be written

$$J(\Delta, \beta, x_\circ) = \frac{\alpha\,\varepsilon^{2/3}}{4\pi}\frac{\ell^{5/3}}{U}\int_{-\infty}^{\infty}\exp\Big(-(x_1\sin\beta + x_\circ\cos\beta)^2\Big)\,\mathrm{e}^{\mathrm{i}\Delta\, x_1\sin\beta}\mathrm{d}x_1$$

$$\int_{-\infty}^{\infty}\left\{1 - \frac{(x_1\sin\beta + x_\circ\cos\beta)^2}{x_\circ^2 + x_1^2 + x_3^2}\right\}\frac{\mathrm{d}x_3}{(x_\circ^2 + x_1^2 + x_3^2)^{11/6}}, \qquad (43)$$

where

$$\Delta = \frac{D}{\ell} \qquad (44)$$

and where $(x_1, x_3) = (k_1\ell, k_3\ell)$ and $x_\circ = \omega/U\ell = k_2\ell$. The integration over x_3 can easily be carried out and (43) is therefore reduced to a single integral

$$J(\Delta, \beta, x_\circ) = \frac{\alpha\,\varepsilon^{2/3}}{4\pi}B\left(\frac{1}{2}, \frac{4}{3}\right)\frac{\ell^{5/3}}{U}\int_{-\infty}^{\infty}\frac{\exp\big(-(x_1\sin\beta + x_\circ\cos\beta)^2\big)}{(x_\circ^2 + x_1^2)^{4/3}}\,\mathrm{e}^{\mathrm{i}\Delta\, x_1\sin\beta}$$

$$\times\left\{1 - \frac{8}{11}\frac{(x_1\sin\beta + x_\circ\cos\beta)^2}{x_\circ^2 + x_1^2}\right\}\mathrm{d}x_1. \qquad (45)$$

In order to obtain the coherence we must normalize $J(\Delta, \beta, x_\circ)$ by

$$J(0, \beta, x_\circ) = \frac{\alpha\,\varepsilon^{2/3}}{4\pi}B\left(\frac{1}{2}, \frac{4}{3}\right)\frac{\ell^{5/3}}{U}\int_{-\infty}^{\infty}\frac{\exp\big(-(x_1\sin\beta + x_\circ\cos\beta)^2\big)}{(x_\circ^2 + x_1^2)^{4/3}}$$

$$\times\left\{1 - \frac{8}{11}\frac{(x_1\sin\beta + x_\circ\cos\beta)^2}{x_\circ^2 + x_1^2}\right\}\mathrm{d}x_1. \qquad (46)$$

and take the absolute square:

$$\mathrm{coh}(\Delta, \beta, \omega D/U) = \left|\frac{J(\Delta, \beta, x_\circ)}{J(0, \beta, x_\circ)}\right|^2. \qquad (47)$$

The integrals (45) and 46) must be calculated by numerical integration and at this point it is advantageous to change variables. We make the substitution $s_\circ = x_\circ\Delta = \omega/U\ell \times D/\ell = \omega D/U$. We change the integration variable similarly by $s = x_1\Delta$. Instead of (45) and (46) we have, respectively

$$J(\Delta,\beta,s_\circ)=\frac{\alpha\,\varepsilon^{2/3}}{4\pi}B\left(\frac{1}{2},\frac{4}{3}\right)\frac{D^{5/3}}{U}\int\limits_{-\infty}^{\infty}\frac{\exp\bigl(-((s\sin\beta+s_\circ\cos\beta)/\Delta)^2\bigr)}{(s_\circ^2+s^2)^{4/3}}\,\mathrm{e}^{\mathrm{i}\,s\sin\beta}$$

$$\times\left\{1-\frac{8}{11}\frac{(s\sin\beta+s_\circ\cos\beta)^2}{s_\circ^2+s^2}\right\}\mathrm{d}s. \qquad (48)$$

and

$$J(0,\beta,s_\circ)=\frac{\alpha\,\varepsilon^{2/3}}{4\pi}B\left(\frac{1}{2},\frac{4}{3}\right)\frac{D^{5/3}}{U}\int\limits_{-\infty}^{\infty}\frac{\exp\bigl(-((s\sin\beta+s_\circ\cos\beta)/\Delta)^2\bigr)}{(s_\circ^2+s^2)^{4/3}}$$

$$\times\left\{1-\frac{8}{11}\frac{(s\sin\beta+s_\circ\cos\beta)^2}{s_\circ^2+s^2}\right\}\mathrm{d}s. \qquad (49)$$

Figure 6 shows examples with six different values of Δ and a selection of angles β.

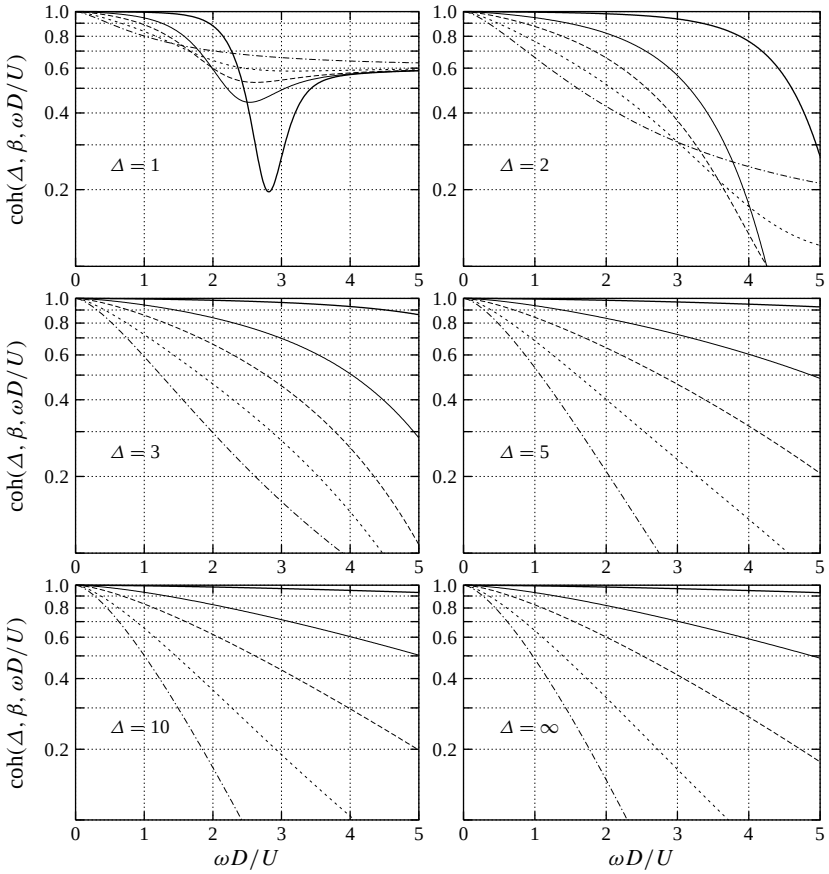

Figure 6. The filtered coherence with six values of $\Delta = D/\ell$. Thick line: $\beta = 1°$, thin line: $\beta = 5°$, dashed line: $\beta = 10°$, short-dashed line: $\beta = 20°$, dot-dashed line: $\beta = 90°$.

4 The Effect of Aliasing

When determining the coherence from a discrete time series by use of digital Fourier transformation it will in general deviate from the coherences predicted by (47) and illustrated in Fig. 6. If the temporal resolution is δt the spectral domain has an upper limit equal to $\omega_N = \pi/\delta t$, the so-called Nyquist frequency or folding frequency [see appendix A and Lumley & Panofsky (1964, p. 53–55)]. Both $J(\Delta, s_\circ)$ in $J(0, s_\circ)$ in (47) are subjected to the operation outlined in (A12) or possibly just (A13) before the aliased coherence is determined. The effect of aliasing is shown in Fig. 7, where the coherences are shown for three different values of Δ and with the dimensionless Nyquist frequency $\omega_N D/U = 5$.

When aliasing and line filtering are both taken into account we get rather complicated results, in particular for small values of Δ . We have worked it out for the same values as in Fig.6 and plotted the coherences with and without aliasing Fig. 7.

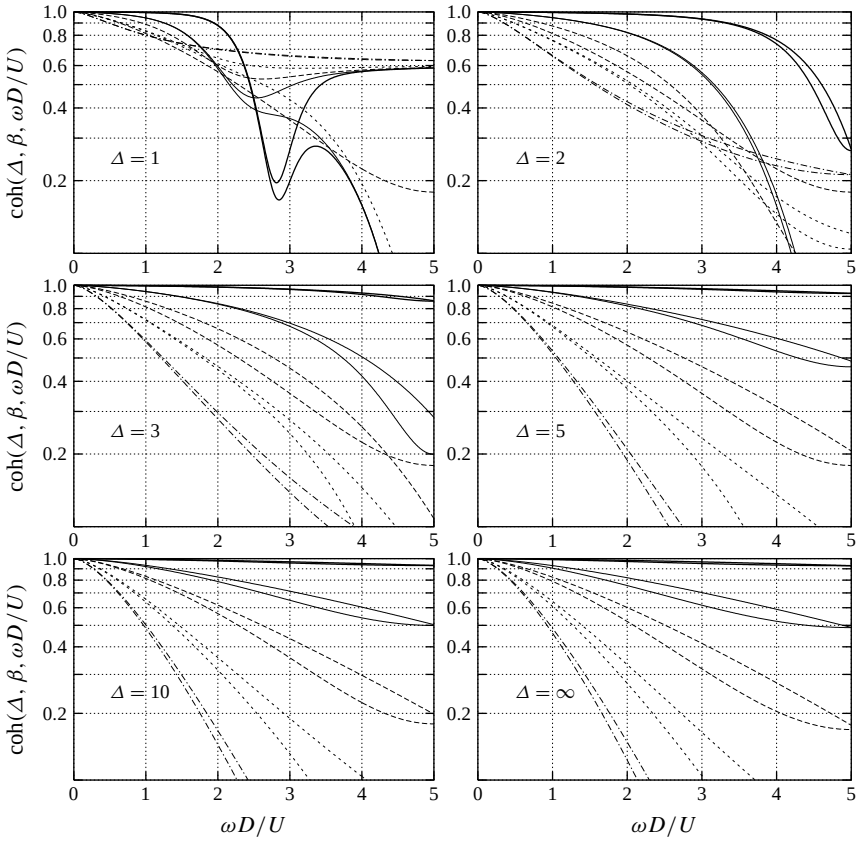

Figure 7. Same as Fig. 6 with aliasing included.

5 Conclusion

We have analyzed the application of a lidar anemometer to obtain, along the beam, the spectral coherence in the mean-flow direction of the along-beam turbulent velocity component. The angle β between the mean-wind direction and the beam is varied between 0 °

and $\pm 90°$. We have observed that theoretically the filtering has a great influence on the measured coherence. More seriously, however, is the effect of aliasing which is caused by the finite time resolution due to the operation of the lidar. The signal from a continuous-wave laser (CW-laser) can, in contrast to the case of the lidar anemometer, be sampled much faster, but since, at the present stage, the laser anemometer is focused at one particular distance it cannot be used to determine spectral coherence along the beam.

The theory discussed here is based on the assumptions that the turbulence is locally isotropic. We have also assumed Taylor's "frozen turbulence" hypothesis which implies that prediction of the longitudinal coherence ($\beta = 0°$) is that it is unity. This prediction is of course not true, but the practical difficulty is that the longitudinal coherence is not easily determined experimentally. The problem is that we don't know the wind direction and thereby β before our sampling period is completed, and at this time it is extremely improbable that the mean-wind direction is such that $\beta = 0°$ within an extremely small margin. It is still to be determined how small this margin is before Taylor's hypothesis "takes over". A semi-quantitative model of longitudinal coherence has been suggested by Kristensen (1979). It is formulated in terms of "eddy turn-over time" and lateral velocity fluctuations and is not particularly useful for predictions.

A Short Story about Aliasing

Consider a pair of time series $x(t)$ and $y(t)$ with zero ensemble means, both of duration T, sampled equidistantly in N points. The time between two neighboring points is $\delta t = T/N$. The two finite, discrete time series are

$$\left\{ \begin{array}{c} x[\ell] \\ y[\ell] \end{array} \right\} = \left\{ \begin{array}{c} x(\ell\delta t) \\ y(\ell\delta t) \end{array} \right\}, \quad \ell = 0, 1, \ldots, N-1. \tag{A1}$$

Their covariance is

$$R_{xy}((\ell'' - \ell')\delta t) \equiv R_{xy}[\ell'' - \ell'] = \langle x[\ell']y[\ell''] \rangle. \tag{A2}$$

For this pair the discrete, finite Fourier transform is

$$\left\{ \begin{array}{c} \widehat{x}[k] \\ \widehat{y}[k] \end{array} \right\} = \frac{1}{N} \sum_{\ell=0}^{N-1} \left\{ \begin{array}{c} x[\ell] \\ y[\ell] \end{array} \right\} \exp(2\pi \mathrm{i}\, \ell k/N), \quad k = 0, 1, \ldots, N-1. \tag{A3}$$

The index k is this equation corresponds to the frequency $\omega_k = k\Delta\omega$ where the spectral resolution is given by

$$\Delta\omega = \frac{2\pi}{T}. \tag{A4}$$

When calculating the the cross spectrum $\psi_{xy}(\omega)$ we assume an ensemble of realizations and form the covariance

$$\psi_{xy}(k\Delta\omega) \equiv \psi_{xy}[k] = \langle \widehat{x}[k]\widehat{y}^*[k] \rangle, \tag{A5}$$

where asterisk means complex conjugation. The covariance can be expressed by $\psi_{xy}(\omega)$ by the relation

$$R_{xy}(\tau) = \int_{-\infty}^{\infty} \psi_{xy}(\omega) \mathrm{e}^{\mathrm{i}\omega\tau} \mathrm{d}\omega. \tag{A6}$$

We insert (A3) in (A5) to obtain

$$\psi_{xy}[k] = \frac{1}{N} \sum_{\ell'=0}^{N-1} \mathrm{e}^{2\pi \mathrm{i} l'k/N} \frac{1}{N} \sum_{\ell''=0}^{N-1} \mathrm{e}^{-2\pi \mathrm{i}\, \ell'' k/N} R_{xy}[\ell'' - \ell']. \tag{A7}$$

Inserting (A6) we get

$$\begin{aligned} \psi_{xy}[k] &= \frac{1}{N} \sum_{\ell'=0}^{N-1} \mathrm{e}^{2\pi \mathrm{i}\, \ell' k/N} \frac{1}{N} \sum_{\ell''=0}^{N-1} \mathrm{e}^{-2\pi \mathrm{i} l'' k/N} \int_{-\infty}^{\infty} \psi_{xy}(\omega) \mathrm{e}^{\mathrm{i}\,\omega(\ell'' - \ell')\delta t} \mathrm{d}\omega \\ &= \int_{-\infty}^{\infty} \psi_{xy}(\omega) \mathrm{d}\omega \left| \frac{1}{N} \sum_{\ell=0}^{N-1} \mathrm{e}^{\mathrm{i}\,\ell(\omega\delta t - 2\pi k/N)} \right|^2 \\ &= \int_{-\infty}^{\infty} \psi_{xy}(\omega) \frac{\mathrm{sinc}^2((\omega - \omega_k)T/2)}{\mathrm{sinc}^2((\omega - \omega_k)\delta t/2)} \mathrm{d}\omega. \end{aligned} \tag{A8}$$

We assume that T is so large that

$$\frac{\mathrm{sinc}^2((\omega-\omega_k)T/2)}{\mathrm{sinc}^2((\omega-\omega_k)\delta t/2)} = \frac{2\pi}{T}\sum_{n=-\infty}^{\infty}\delta(\omega-\omega_k+n2\pi/\delta t). \tag{A9}$$

With this Dirac delta-comb we get

$$\psi_{xy}[k] = \Delta\omega\sum_{n=-\infty}^{\infty}\psi_{xy}(\omega_k+n2\pi/\delta t). \tag{A10}$$

We see that $\psi_{xy}(\omega_k)$ is periodic with the period $2\pi/\delta t$ and we therefore usually confine us to the interval $|\omega_k| \le \omega_N$, where $\omega_N = \pi/\delta t$ is the Nyquist frequency.

We may reformulate (A10) by writing $\psi_{xy}(\omega)$ as

$$\psi_{xy}(\omega) = C_{xy}(\omega) + \mathrm{i}\, Q_{xy}(\omega), \tag{A11}$$

where $C_{xy}(\omega)$ and $Q_{xy}(\omega)$ are the even co-spectrum and the odd quadrature-spectrum, respectively. Then

$$\begin{aligned}\frac{\psi_{xy}[k]}{\Delta\omega} &= C_{xy}(\omega_k) + \mathrm{i}\, Q_{xy}(\omega_k)\\ &\quad + \sum_{n=1}^{\infty}\left\{C_{xy}(2n\omega_N+\omega_k) + C_{xy}(2n\omega_N-\omega_k)\right\}\\ &\quad + \mathrm{i}\sum_{n=1}^{\infty}\left\{Q_{xy}(2n\omega_N+\omega_k) - Q_{xy}(2n\omega_N-\omega_k)\right\}\end{aligned} \tag{A12}$$

Usually it is sufficient to truncate the summations and use the approximation

$$\frac{\psi_{xy}[k]}{\Delta\omega} \simeq \left(C_{xy}(\omega_k) + C_{xy}(2\omega_N-\omega_k)\right) + \mathrm{i}\,\left(Q_{xy}(\omega_k) - Q_{xy}(2\omega_N-\omega_k)\right). \tag{A13}$$

Acknowledgements

The authors are grateful for the support to the WindScanner project from the Danish Strategic Research Council.

References

Banakh, V. A. & Smalikho, I. N. (1997), 'Estimation of the turbulence energy dissipation rate from the pulsed doppler lidar data', *Atmos. Oceanic Opt.* **10**, 957–965.

Frehlich, R. (1997), 'Effects of wind turbulence on coherent doppler lidar performance', *J. Atmos. Ocean. Technol.* **14**, 54–75.

Kristensen, L. (1979), 'On longitudinal spectral coherence', *Boundary-Layer Meteorol.* **16**, 145–153.

Kristensen, L. & Jensen, N. O. (1979), 'Lateral coherence in isotropic turbulence and in the natural wind', *Boundary-Layer Meteorol.* **17**, 353–373.

Kristensen, L., Lenschow, D. H., Kirkegaard, P. & Courtney, M. S. (1989), 'The spectral velocity tensor for homogeneous boundary-layer turbulence', *Boundary-Layer Meteorol.* **47**, 149–193.

Lumley, J. L. & Panofsky, H. A. (1964), *The Structure of Atmospheric Turbulence*, John Wiley & Sons, Inc., New York.

Olver, F. W. J. (1964), Bessel functions of integer order, *in* M. Abramowitz & I. Stegun, eds, 'Handbook of Mathematical Functions with Formulas, Graphs, and Mathematical Tables. Gamma Function and Related Functions', Applied Mathematics Series 55, National Bureau of Standards, chapter 9, pp. 355–433.

Risø DTU is the National Laboratory for Sustainable Energy. Our research focuses on development of energy technologies and systems with minimal effect on climate, and contributes to innovation, education and policy. Risø has large experimental facilities and interdisciplinary research environments, and includes the national centre for nuclear technologies.

Risø DTU
National Laboratory for Sustainable Energy
Technical University of Denmark

Frederiksborgvej 399
PO Box 49
DK-4000 Roskilde
Denmark
Phone +45 4677 4677
Fax +45 4677 5688

www.risoe.dtu.dk